

EXTRATERRESTRIAL NOISE IN THE UHF REGION (300-3,000 Mc) (NOISE FROM THE MOON)

N65-36437

FACILITY FORM 602	(ACCESSION NUMBER)	(THRU)
	35	1
	(PAGES)	(CODE)
	DR 67493	07
	(NASA CR OR TMX OR AD NUMBER)	(CATEGORY)

JANUARY 1965

GPO PRICE \$ _____

CSFTI PRICE(S) \$ _____

Hard copy (HC) 2.00

Microfiche (MF) .50

EXTRATERRESTRIAL NOISE IN THE
UHF REGION (300-3,000 Mc)
(NOISE FROM THE MOON)

by

Herbert Martinides

JANUARY 1965

The author is a member of the European Space Research Organization, European Space Technology Center, Delft, Holland, and worked at the Goddard Space Flight Center for one year.

Goddard Space Flight Center
Greenbelt, Md.

CONTENTS

	Page
ABSTRACT	vi
PROBLEM	1
CONSTANTS	1
Moon	1
Sun	1
PHYSICAL CONSTANTS	2
DEFINITIONS AND BASIC LAWS	2
Flux Density	2
Surface Brightness	2
Planck's Law for a Black Body	2
Rayleigh-Jeans Law	2
RADIATION SOURCES	3
THERMAL RADIATION FROM THE MOON	3
REFLECTION OF RADIATION BY THE MOON SURFACE	
AT 2,000 MC	5
Radioechos from the Moon	5
Reflection of Waves from the Sun or Other Sources by the Moon	7
THERMAL RADIATION FROM THE QUIET SUN	8
RADIATION FROM THE ACTIVE SUN	9
Thermal Radiation from Centers of Activity	9
Non-Thermal Radiation	11
Large Flare Events	13
Small Flare Event	13
Conclusion (about flux density or bursts)	14

	Page
GALACTIC RADIO EMISSION	14
The Continuum.	14
DISCRETE SOURCES OF COSMIC RADIO WAVES	20
Within the Galaxy.	20
External Galaxies.	21
Radio Emission from Clusters of Galaxies	22
Conclusion about Discrete Sources	22
REFLECTION OF COSMIC RADIO WAVES ON THE MOON	
SURFACE.	22
Continuum	22
Discrete Sources	24
FINAL REMARKS	24
REFERENCES	25
APPENDIX I.	27

LIST OF ILLUSTRATIONS

Figure	Page
1 Lunar temperature	3
2 Radio observations of the brightness temperature of the central portion of the lunar disk	4
3	5
4	6
5 Radiospectrum of the Sun for spot maximum and minimum ...	8
6	9
7	10
8 Annual mean sunspot numbers for 1749 to 1957; for 1609 to 1749 only the epochs of maxima and minima and the approximate maximum sunspot numbers are known. The highest maximum since 1610 occurred in 1957	10
9 Tentative spectra of the peak intensities of outburst (Type II burst) and of stormbursts (Type I bursts) as compared with the spectrum of the quiet Sun	11

Figure		Page
10	Spectra of Type III bursts	12
11	Idealized model of the spectrum of a complete radio outburst, showing the different possible components of the Type IV burst	13
12	Distribution of radiation of 50 cm wavelength (Piddington and Trent). Coordinates are right-ascension and declination for 1955; a few galactic longitudes have been indicated	16
13a	A fragment of the galactic map made by Hill, Slee, and Mills on 3.5 m. The contour unit is 1000°K	17
13b	The same region of the galaxy as shown in Figure 13a to the same scale as observed on 22 cm by Westerhout. The contour unit is 3.25°K. Compare the two maps in the regions of the galactic center (longitude 327.7°); also note the large number of discrete sources superimposed on the background, some of which appear on both maps	17
14	A chart to convert from equatorial to galactic coordinates or vice versa (epoch 1900)	18
15	Diagram, due to Plaskett, illustrating the size and shape of the galaxy and the position of the sun. The large white dots represent the globular clusters (Rudaux and de Vaucouleurs, 1948)	18
16	Intensity of general cosmic radio emission [1, 7, 11, 12]. General galactic radio emission is concentrated along the galactic equator and towards the galactic center. Measurements are disturbed by irregularities and superimposed sources. We chose as representative regions the galactic ridge at $l^{II} = \pm 10^\circ$ (i.e. avoiding the Sgr A source), and the coldest part of the sky near $b^{II} = \pm 90^\circ$	19
17	19
18	Provisional radio-frequency spectra of the four principal sources as compiled by Wild	21
19	22
20	28
21	29
22	30
23	30

ABSTRACT

36437

This survey is a result of a study of the available literature about extraterrestrial noise. It has been attempted to select the most reliable and significant data and sources through 1962, 1963. Numerical values about the extraterrestrial noise were considered here. For this reason any theory and speculation about this radiation has been omitted. The lack of experimental data is sometimes significant, but they are supplemented continuously by the great efforts on this subject at the present time.

As noise sources were considered the radiation of the moon, sun, galactic structures (interstellar hydrogen, and high energy electrons in the interstellar magnetic field), discrete sources and radiation from outside our galaxy.

In particular the amount of noise, received by an antenna (2,000 Mc) pointed to the moon has been evaluated:

author

Thermal Radiation from the Moon

Minimum: $8 \cdot 10^{-24}$ W/m² cycle (T = 100°K)

Maximum: $3.1 \cdot 10^{-23}$ W/m² cycle (T = 390°K)

Reflected Thermal Radiation from the Quiet Sun

Sun Spot Minimum: $2.3 \cdot 10^{-27}$ W/m² cycle

Sun Spot Maximum: $2.9 \cdot 10^{-27}$ W/m² cycle

slow varying component (~ 27 days): $\sim 3 \cdot 10^{-27}$ W/m² cycle
cm bursts; top intensity in the same order as the quiet sun' level. Average value: $\approx 2 \cdot 10^{-29}$ W/m² cycle.

Reflected Radiation from the Active Sun

$\approx 4 \cdot 10^{-26}$ W/m² cycle—(10^{-23} W/m² cycle questionable) 20-40 minutes increase, decay several hours.

Reflected Radiation from the Galactic Continuum

$\approx 10^{-26}$ W/m² cycle

Reflected Radiation from all Discrete Sources

$\approx 6 \cdot 10^{-30}$ W/m² cycle.

EXTRATERRESTRIAL NOISE IN THE UHF REGION
(300-3,000 Mc)

by

Herbert Martinides

PROBLEM

An antenna, tuned to 2,000 Mc, is pointed to the moon. The amount of noise which the antenna receives, and the origin of it, should be investigated.

CONSTANTS

Moon

Radius: $r = 1,738 \text{ km}$

Mean distance earth/moon: $d = 3.84 \cdot 10^5 \text{ km}$

Surface of the moon: $3.8 \cdot 10^7 \text{ km}^2$

Eccentricity of moon orbit: 0.054

Mean temperature of moon surface: 374°k

Plane of moon orbit inclined 6° against ecliptic. Angular diameter: $\sim 0.5^\circ$

Sun

Radius: $r = 6.9 \cdot 10^5 \text{ km}$

Mean distance earth/sun: $1.5 \cdot 10^8 \text{ km}$

Perihel: 147,156,000 km

Aphelia: 152,169,000 km

Steradians:

Perihel: 0.00007034

Aphelia: 0.00006580

Square Degree:

Perihel: 0.2309

Aphelia: 0.2156

Angular diameter: $\sim 0.5^\circ$

PHYSICAL CONSTANTS

Planck's constant: $h = 6.625 \cdot 10^{-27}$ erg.sec.

Boltzmann's constant: $k = R/L = 1.38 \cdot 10^{-16}$ erg.deg.⁻¹

Velocity of light: $c = 2.9979 \cdot 10^{10}$ cm/sec.

DEFINITIONS AND BASIC LAWS

Flux Density: $S = \frac{\Delta E}{\Delta A \Delta t \Delta V}$

(ΔE = energy)

(ΔA = emitting area)

(Δt = time)

(ΔV = frequency bandwidth)

(erg/cm² sec cycle bandwidth)

Surface Brightness: $B = \lim_{\Delta\Omega \rightarrow 0} \Delta S / \Delta\Omega$

(erg/cm² sec cycle bandwidth, steradian)

The brightness temperature T (°K) follows from (1) or (2).

Planck's Law for a Black Body:

$$B_v = \frac{2 h \nu^3}{c^2 \exp (h\nu/kT - 1)} \quad (1)$$

Rayleigh-Jeans Law:

$$B_v = \frac{2k T \nu^2}{c^2} h\nu \ll kT \quad (2)$$

ν = frequency of the radiation

RADIATION SOURCES

Thermal Radiation from the Moon.

Direct or on the Moon Surface Reflected Radiation.

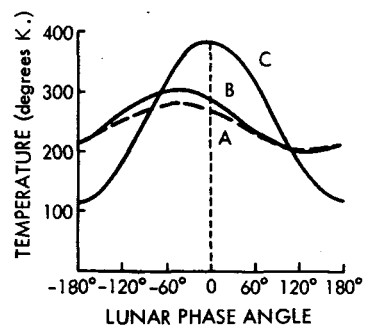
1. Thermal radiation from the quiet sun.
2. Radiation from the active sun.
3. Radiation from galactic structures.
4. Discrete sources.
5. External galaxies.

In the following each of these sources will be considered for the UHF region, but especially for 2.000 Mc. It should be kept in mind that the results of measurement at 1.430 Mc ($\lambda = 21,1$ cm) may not be extrapolated to 2.000 Mc, since there is a hyperfine structure line of atomic hydrogen at this frequency.

THERMAL RADIATION FROM THE MOON

The temperature of the lunar surface taken from reference 1 is shown by Figure 1.

Figure 1—Lunar temperature curves. (a) Average microwave temperature over the moon's disk. $T = 239 + 40 \cdot 3 \cos(\omega t - 1/4\pi)$. (b) Microwave temperature of the center of the disk. $T = 249 + 52 \cdot 0 \cos(\omega t - 1/4\pi)$. (c) Fundamental component of the infrared temperature variation at the center of the disk. $T = 249 + 134 \cos \omega t$.



The striking feature of Figure 1 is the much less variation of the temperature during a lunar cycle for microwaves than for infrared. Also the maximum is occurring later than that for infrared. This all is explained by heat conduction and the fact that the emitting layer is in the order of wave length. For infrared this is in the order microns, for microwaves in the order of decimeters.

More complete summaries are given in References 2 and 10.

In Figure 2 the results of temperature measurements during a lunar cycle are plotted.

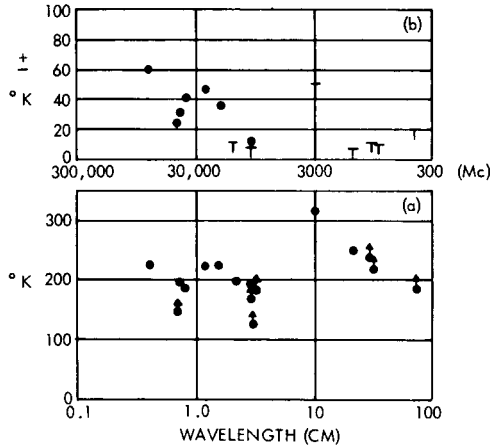


Figure 2—Radio observations of the brightness temperature of the central portion of the lunar disk from the data of Table 1. Abscissae: wavelength in cm (logarithmic scale); ordinates: apparent temperature (°K). (a) Constant component; (b) variable component. Average (disk) to center of disk corrections shown as arrows (a).

There exists a considerable spread of the values. It is, however, possible to establish an upper and lower limit, that is:

$$T_{\max} = 360^{\circ}\text{K} \quad T_{\min} = 100^{\circ}\text{K}$$

The radio brightness temperature at the center of the moon's disk is about 210°K.

The flux density S and the surface brightness B_v are connected by the known relation:

$$S \doteq \pi B_v r^2 / d^2 \quad (3) \quad d = \text{distance}$$

$$S = B_v \Omega \quad r = \text{radius of the radiating disk} \quad (3)$$

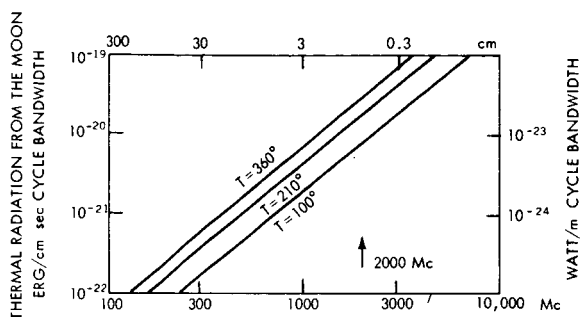
$$\Omega = \text{solid angle (steradians), } 6 \cdot 10^{-5} \text{ for moon}$$

Substituting the values for the moon (3) yields:

$$S = 2.10^{-41} T_v^2 \text{ (erg/cm}^2 \text{ sec cycle bandwidth)}$$

Figure 3 shows the energy flux S_m on the earth surface from the moon, generated by thermal radiation, as a function of the frequency.

Figure 3



For 2,000 Mc we have:

$$T = 100^{\circ}\text{K}; S_m = 8.10^{-21} \text{ erg/cm}^2 \text{ sec cycle bandwidth}$$

$$T = 390^{\circ}\text{K} S_m = 3.1.10^{-20} \text{ erg/cm}^2 \text{ sec cycle bandwidth}$$

REFLECTION OF RADIATION BY THE MOON SURFACE AT 2,000 MC

Radioechos (Reference 3) from the Moon.

The echo cross section σ is defined by $S_r = \sigma S_i / 4\pi d^2$

S_r = receiving flux density at the distance d

S_i = incident flux density.

It is convenient to split σ into three factors:

$$\sigma = A \rho D \tag{4}$$

A = effective projected reflecting area.

ρ = power reflection coefficient (Appendix 1)

Evans (Reference 7) reports a $\rho = 0,1$ (120 Mc).

Reference 3 states $\rho = 0,1-0.15$ by analogy with terrestrial materials.

Figure 4 gives the power reflection coefficients as a function of the dielectrical constant ϵ_r for a dielectrical material.

The data of ρ , mentioned above, would imply a $\epsilon_r = 4-6$ (see Appendix 1).

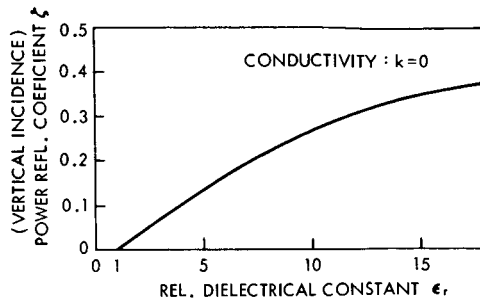


Figure 4

D = directivity (Reference 3).

D = 1 for a smooth sphere

D = 2,7 perfectly rough sphere

Evans (Reference 7) gives the values D = 1,8 for his experiments at 120 Mc. For comparison it is mentioned that D = 5,7 for the optical region.

Various measurements of the echo cross section have been performed at various frequencies and other conditions (References 3, 7, 8, 9 and 10).

The results demonstrate that the moon surface is quasispecular in the frequency region 120 Mc-2860 Mc with some dependence on the frequency. All this means, that the moon has irregularities, smaller and greater, as compared with the wave length ($\lambda = 10-250$ cm).

But we are interested in the echo cross section σ for a continuous wave. Trexler (Reference 8) made a study of the transmission loss for cw (earth-moon-earth) and found his value in good agreement with that of other experimenters. He concluded from all available data to him, that the transmission loss for cw increases about 6db per octave in the region from 30-3000 Mc, being, 258 db at 300 Mc. Isotropic transmitting and receiving antennas are assumed. The uncertainty is 4 db.

Applying the well-known formula,

$$P_{out} = \frac{P_{in} \cdot G_r}{4\pi d^2} \cdot \frac{\sigma}{4\pi d^2} \cdot \frac{G_r \cdot \lambda^2}{4\pi}$$

Substituting the constants:

$$\sigma \text{ (km}^2\text{)} = 4,8 \cdot 10^{26} \cdot \text{frequency}^2 \text{ (Mc)} \cdot P_{out} / P_{in}$$

using the values for the transmission loss from Trexler, becomes:

$$\underline{\sigma \doteq 7.10^5 \text{ km}^2} \text{ for continuous wave 30-3000 Mc}$$

According to the given uncertainty of 4 db, the true value of σ should lie between $1,7.10^5 - 2,7.10^6 \text{ km}^2$.

A further consequence of Trexler's data is that σ is independent of the frequency between 30 and 3000 Mc.

$$\text{Moon Disk: } 10^7 \text{ km}^2$$

Reflection of Waves from the Sun or Other Sources by the Moon

In order to obtain the flux density on the earth surface of reflected radiation by the moon, the flux density at the moon surface has to be multiplied by a factor $\sigma^1/4\pi d^2$. (d = distance earth/moon, σ^1 = reflection cross section.)

Full Moon. For this special case the reflection cross section is in principle the same as the radar cross section, discussed in the previous chapter. Using this result $\sigma/4\pi d^2$ becomes

$$\underline{\sigma/4\pi d^2 = 3,8.10^{-7}}$$

with the true value lying between $1.10^{-7} - 1,5.10^{-6}$.

Substituting the values given by Evans (Reference 7) S = 0, 1, D = 1.8 yields $\sigma/4\pi d^2 = 10^{-6}$.

For visible light:

$$\sigma/4\pi d^2 = 1,7.10^{-6}$$

$\sigma/4\pi d^2$ During the Lunar Cycle. The factor $\sigma/4\pi d^2$ is the largest for full moon. For the other part of the lunar cycle $\sigma/4\pi d^2$ is smaller because:

1. The visible illuminated area A_m is smaller:

$$A_m = r^2 \pi |\sin \pi t/T|$$

(r = radius of the moon)
 (T = time of the lunar cycle).

2. The reflection in any other direction than perpendicular is smaller.
 (Appendix I.)

At this point it is of interest that F. G. Smith challenged the auditorium to detect reflected waves from the sun (1959, Reference 10), which has not been done until this time.

THERMAL RADIATION FROM THE QUIET SUN

The microwave radiation of the thermal sun is generated in the hot gas in the surrounding corona. The mechanism of emission is the following: An electron passes a proton and suffers an acceleration (Reference 3). The brightness for microwave is not uniformly distributed across the sun. It shows a maximum at about the limb, depending on the frequency (Reference 12).

Figure 5 shows the radiospectrum for the quiet sun:

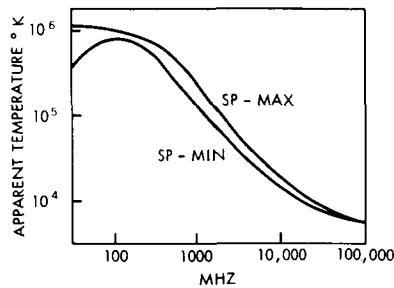


Figure 5—Radiospectrum of the Sun for spot maximum and minimum. C. W. Allen: Monthly Notices Roy. Astronom. Soc. London 117, 174 (1957).

The energy flux S_q from the sun on the earth surface can be calculated by formulas 2 and 3 and by Figure 5:

$$S_q \doteq 2 \cdot 10^{-41} v^2 T \text{ (erg/cm}^2 \text{ sec cycle bandwidth)} \quad (5)$$

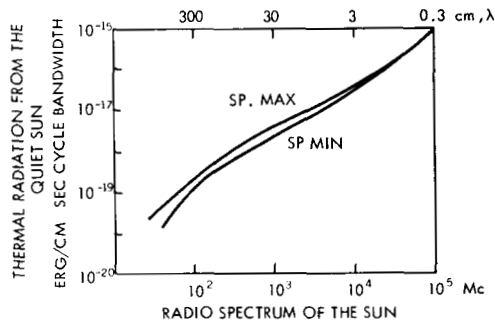
Figure 6 shows a plot of these data.

The numerical values for 2000 Mc are:

For spot maximum $S_q \doteq 7.7 \cdot 10^{-18}$ erg/cm² sec cycle bandwidth

For spot minimum $S_q \doteq 6 \cdot 10^{-18}$ erg/cm² sec cycle bandwidth

Figure 6



The reflected energy flux S_{qr} during full moon is then:

$$S_{qr} = S_q \cdot \sigma / 4\pi d^2$$

For 2,000 Mc:

For spot maximum: $S_{qr} \doteq 2.9 \cdot 10^{-24}$ erg/cm² sec cycle bandwidth

For spot minimum: $S_{qr} \doteq 2.3 \cdot 10^{-24}$ erg/cm² sec cycle bandwidth.

These values are more than a factor 10^4 less than these for the thermal radiation of the moon.

The physical reality of the model of a quiet sun is questionable.

RADIATION FROM THE ACTIVE SUN

Thermal Radiation from Centers of Activity (Reference 3)

α . Slow Varying Component (~ 27 Days). Coronal activity centers (radio condensations) are the origin of this radiation and probably simply represents the thermal emission of regions with higher density and temperature than normal.

This radiation is associated with faculae of the sun, not with the associated sun spot groups. They are 40,000-100,000 km higher than the faculae and they seem to be flat, at least for certain wavelength regions. The average lifetime is several months. The average area amounts to several minutes of arc. The temperature lies in the order of 10^6 K. Maximum temperature is $2 \cdot 10^6$ K. Measurements have been reduced to the sun spot area $A = 2 \cdot 10^{-3}$ of the hemisphere, to the number of sunspots $R = 100$, and to the facular area $F = 2 \cdot 10^{-3}$ of the hemisphere. The flux density for $A = 2 \cdot 10^{-3}$, or $F = 2 \cdot 10^{-3}$ or $R = 100$ is more or less the same.

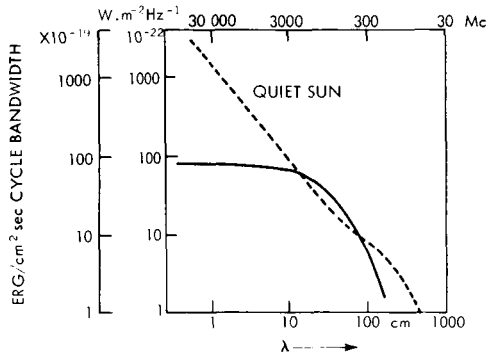


Figure 7—Solid line: Tentative spectrum of the 27 days component, for a sunspot area $A = 2 \times 10^{-3}$ visible hemisphere. For comparison the quiet Sun spectrum is given by a dotted line.

Figure 7 shows a tentative spectrum of the slowly fluctuating component. The curve would have the same shape if there were 100 sunspots as it already was stated or the faculae area was $2 \cdot 10^{-3}$ of the solar disc.

The important conclusion from this figure is, that the influence of the slow varying component is the most significant in the frequency range 300 Mc-3000 Mc. The total energy flux can be more than twice the flux of the quiet sun, depending on the activity of the sun. The following Figure 8 gives the annual mean sunspot number for a number of the 11 year-solar cycles. The peak value of sunspots during 1947 was 320 sunspots, the minimum value 40.

β . Bursts at Centimeter-Wave Lengths (Reference 3). 90% of these bursts ($\lambda < 20$ cm) are rather smooth. Often they seem to decay exponentially with a decay time of 10-20 minutes. Their top intensities are of the same magnitude as the quiet sun's level.

Their origin is probably the thermal radiation emitted by flare regions. So their region of origin is an area of about ≈ 1 inch in diameter.

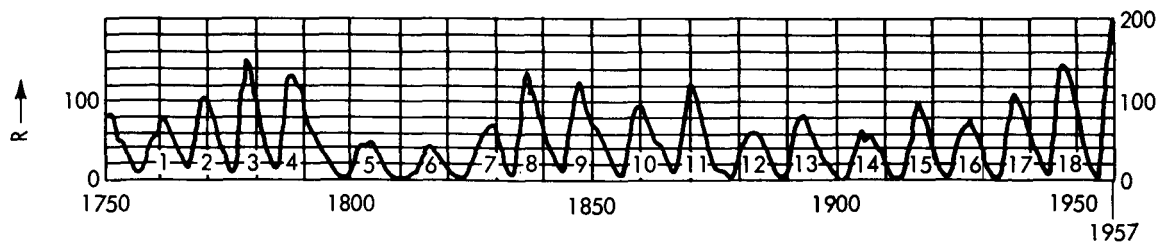


Figure 8—Annual mean sunspot numbers for 1749 to 1957; for 1609 to 1749 only the epochs of maxima and minima and the approximate maximum sunspot numbers are known. The highest maximum since 1610 occurred in 1957. (See M. Waldmeier: Ergebnisse und Probleme der Sonnenforschung, 2nd ed., p. 151, Leipzig 1955. Additional R-values for 1954 onward are taken from the annual Zurich reports.)

Non-Thermal Radiation (References 3, 12, and 13)

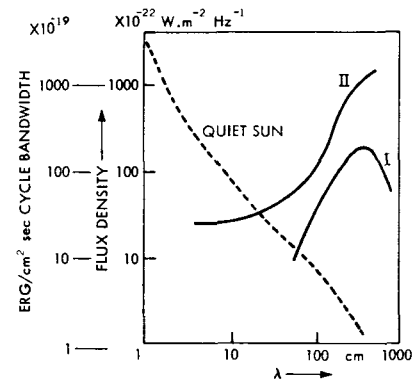
This kind of radiation consists of varying emissions (bursts) with durations of some seconds or less, until hours. These bursts are conveniently classified by their duration, polarization, bandwidth and their associated optical features (Types I-V).

In the following only a very rough survey is given:

Type I—Noise Storms

- Duration: Hours to days, consists of many short pulses (≈ 1 sec.), e.g., at 200 Mc, half width 0,3-0,4 sec., 900 Mc, half width 0,2 sec. (rare).
Diameter: Minutes of arc.
Spectrum: Below ~ 30 Mc. (See Figure 9.)
Apparent temperature: $\sim 10^9$ K.
Origin: Cerenkov radiation

Figure 9—Tentative spectra of the peak intensities of outburst (type II burst) and of stormbursts (type I bursts) as compared with the spectrum of the quiet Sun. Slightly changed, after a compilation by R. Coutrez (Radio astronomie).



Type II

- Duration: Minutes—tens of minutes.
Spectrum: See Figure 9. Frequency drifts towards lower frequencies with a rate 0.1 Mc/sec.
Apparent Temperature: 10^{11} K.
Origin: Follows the start of a flare, due to shock wave.

Type III Burst

- Duration: Seconds. Often in groups with a rate 10-100 per hour.
Diameter: Up to $(10')^2$ increasing with wave length.
Spectrum: Below 300 Mc, fast drift. (See Figure 10.)

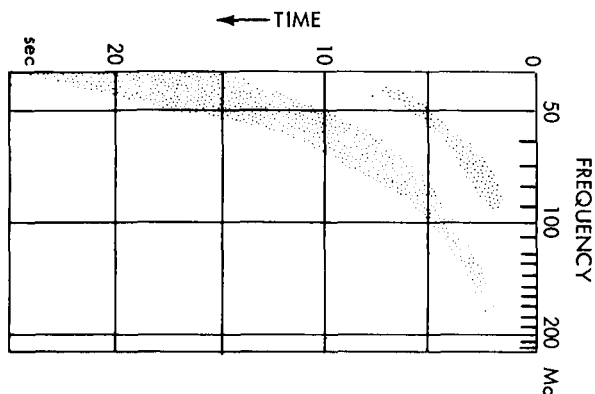


Figure 10—Spectra of Type III bursts. Abscissa: frequency in MHz; ordinate: time in seconds.

Apparent Temperature: $> 10^{11}$ K.

Origin: Probably periodic oscillations of the coronal plasma. Source moves upwards through corona, sometimes exceeding 10^5 km/sec. estimated flux density S_{III} : using $T = 10^{11}$, angular diameter $10'$: $S_{III} \sim 2 \cdot 10^{-14}$ erg/cm² sec cycle bandwidth at 100 Mc.

No exact data were available.

Type IV

Duration: Occurs always after a flare; intensity increases during 20-40 minutes and decreases slower (one or several hours).

Diameter: Up to $10'$ increasing with wave length, source diameter: 150,000-350,000 km.

Spectrum: Continuous, occurring in the range mainly ≈ 500 -1000 Mc, cut off below 500 Mc.

Apparent Temperature: $\sim 10^{11}$ K.

Origin: Type IV is connected with Type II bursts, synchrotron radiation, associated with cosmic rays.

Flux Density S_{IV} : Only one value could be found (Reference 3):
 $S_{IV} = 10^{-16}$ erg/cm² cycle bandwidth sec.

Using $T = 10^{11}$ K, source diameter $3,5 \cdot 10^5$ km.

$S_{IV} = 3 \cdot 10^{-14}$ erg/cm² sec cycle bandwidth for 500 Mc.

Type V

Duration: Minutes

Diameter: Large

Spectrum: Below 100 Mc. Bandwidth some tens of Mc.

Apparent Temperature: $\sim 10^{11}$ K.

Origin: Similar to Type IV bursts, occur together or shortly after Type III bursts.

Flux Density: Reach intensities up to 10^{-15} erg/cm² cycle bandwidth.

Large Flare Events

In this case an idealized model of a complete radio outburst was constructed (Figure 11). All types of bursts appear.

Small Flare Event

The commonest type of isolated burst is Type III and can accompany the smallest of optical flares.

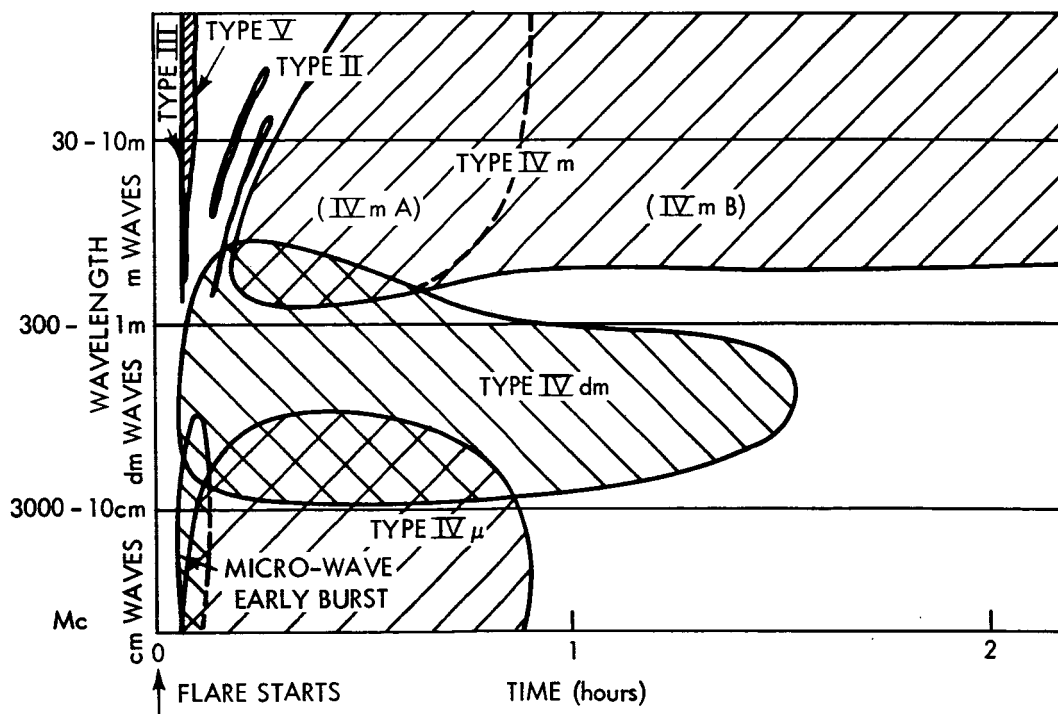


Figure 11—Idealized model of the spectrum of a complete radio outburst, showing the different possible components of the Type IV burst (Kyoto conference, 1961).

Conclusion (about flux density of bursts)

Lack of experimental data and the matter itself make it difficult to provide very reliable figures for the flux density at a given frequency.

But about 300 Mc, only Type IV can be expected to be significant. As it was already mentioned, the flux density is in the order of:

$$S_{IV} \sim 10^{-16} \text{ erg/cm}^2 \text{ sec cycle bandwidth.}$$

$$(\sim 3 \cdot 10^{-14} \text{ erg/cm}^2 \text{ sec cycle bandwidth.})$$

can be expected, the latter being properly an upper limit.

The reflected flux density during full moon would then be:

$$S_{IV}^r \sim 4 \cdot 10^{-23} \text{ erg/cm}^2 \text{ sec cycle bandwidth.}$$

$$(S_{IV}^r \sim 1 \cdot 10^{-20} \text{ erg/cm}^2 \text{ sec cycle bandwidth.})$$

The last figure still being a factor 3 lower than the maximal thermal radiation from the moon in the radio frequency region.

GALACTIC RADIO EMISSION

The Continuum (References 12 and 15)

Our own galaxy emits radiation in the radio frequency region, depending strongly on the wave length. These radio galaxies are very bright on meter waves, and narrow and fainter on decimeter waves, suggesting distinct mechanisms. A powerful emitting region in the constellation Sagittarius shows that radio waves are absorbed much less than light. (In Sagittarius the center of our galaxy is situated.) On the other hand absorbing matter darkens parts of the radio galaxy, (e.g., between Cygnus and Sagittarius).

The meter wave radiation is due to high energy electrons in a magnetic field (non-thermal).

On decimeter wave lengths a good part of the radiation comes from a highly concentrated zone along the galactic plane, even narrower than the narrow component on meter wave length. The origin of this radiation is thermal emission from ionized interstellar hydrogen.

From these mechanisms it appears that the whole sky is not "dark" for radio waves, but illuminated because the earth is situated near the galactic plane. The center of our galaxy ($\alpha = 17^{\text{h}} 42^{\text{m}}.4 = 265^{\circ}36'$ $\delta = -28^{\circ}55'$, 1950) appears as the brightest region, of which maps are given in Figures 11 and 12.

The galactic coordinate system: The latest definition is given in Figure 13 (1960). At this time conversion tables should be prepared for celestial coordinates. It is not known if these are already available.

I.A.U. galactic coordinate system $l^{\text{II}}, b^{\text{II}}$ [6]. Galactic pole ($b^{\text{II}} = +90^{\circ}.0$).

$$\alpha = 12^{\text{h}} 46^{\text{m}}.6 = 191^{\circ} 39' \quad \delta = +27^{\circ} 40' \quad (1900)$$

$$\alpha = 12^{\text{h}} 49^{\text{m}}.00 = 192^{\circ} 15' \quad \delta = +27^{\circ} 24'.0 \quad (1950)$$

$$l^{\text{I}} = 347^{\circ} 40' \quad b^{\text{I}} = +88^{\circ} 31'$$

Point of zero longitude and latitude ($l^{\text{II}} = 0, b^{\text{II}} = 0$) [6]. This point agrees with the position of the galactic center

$$\alpha = 17^{\text{h}} 39^{\text{m}}.3 = 264^{\circ} 50' \quad \delta = -28^{\circ} 54' \quad (1900)$$

$$\alpha = 17^{\text{h}} 42^{\text{m}}.4 = 265^{\circ} 36' \quad \delta = -28^{\circ} 55' \quad (1950)$$

For a quick conversion Figure 14 is given. These older galactic coordinates designate the galactic center with $l = 330^{\circ}$. Figure 15 shows the position of the sun in the galaxy.

At the present state of the art, it is not possible to give a complete map for the radio emission for every frequency. However, it is possible to give the flux density for the galactic pole as the coldest spot and for the galactic equator as the hottest spot as a function of frequency. (Figure 16)

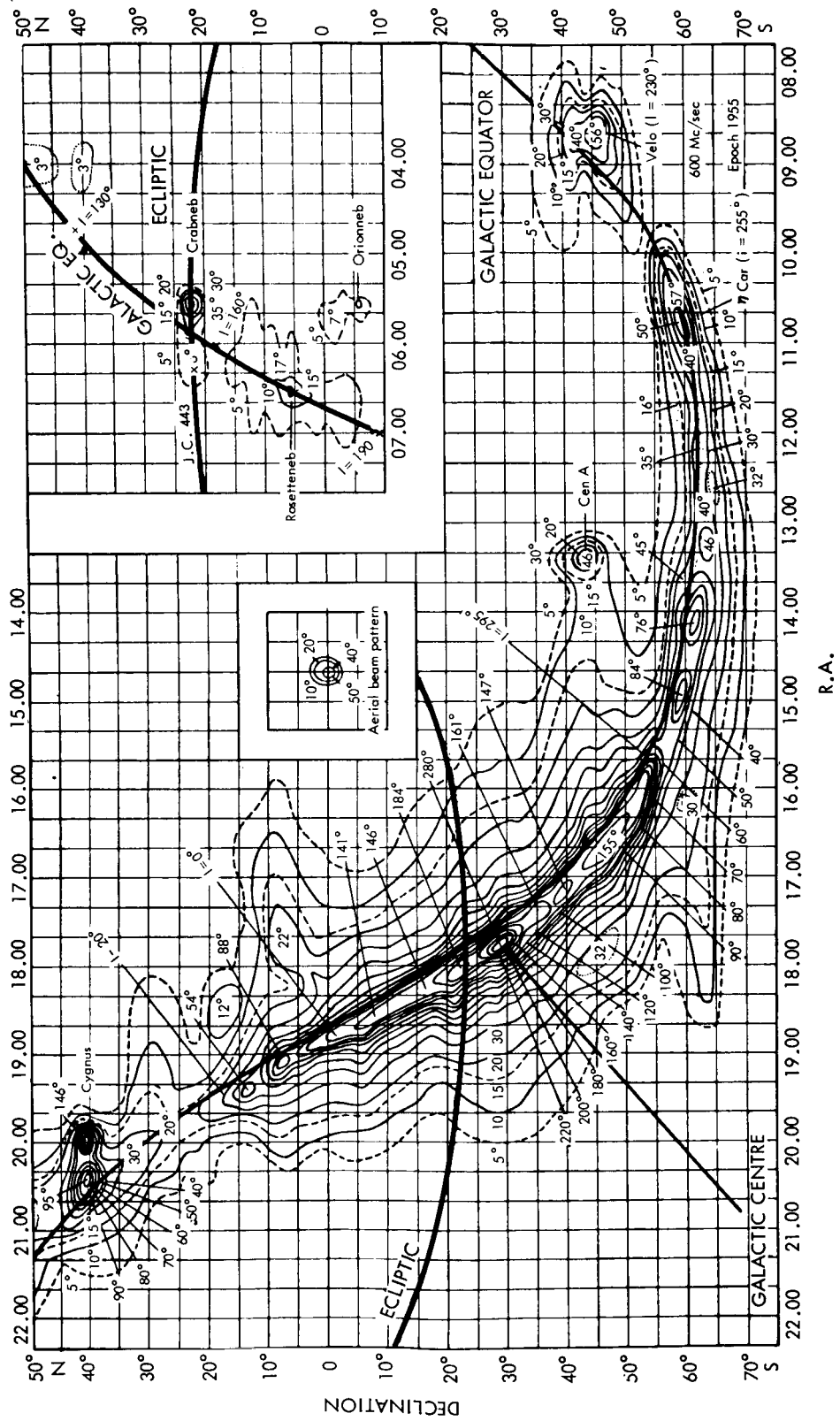


Figure 12—Distribution of radiation at 50 cm wavelength (Piddington and Trent). Coordinates are right-ascension and declination for 1955; a few galactic longitudes have been indicated.

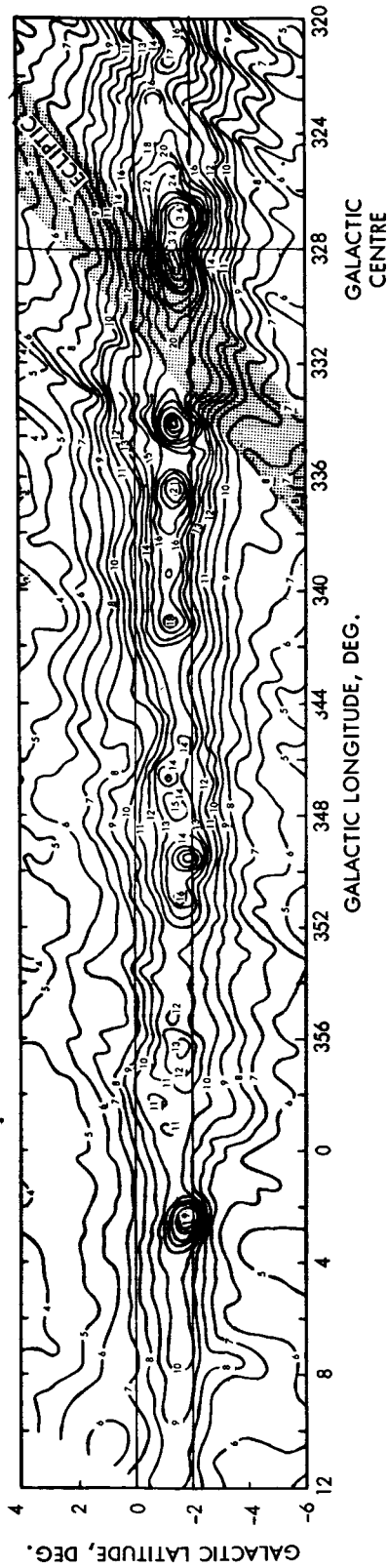


Figure 13a—A fragment of the galactic map made by Hill, Slee, and Mills on 3.5 m. The contour unit is 1000° K.

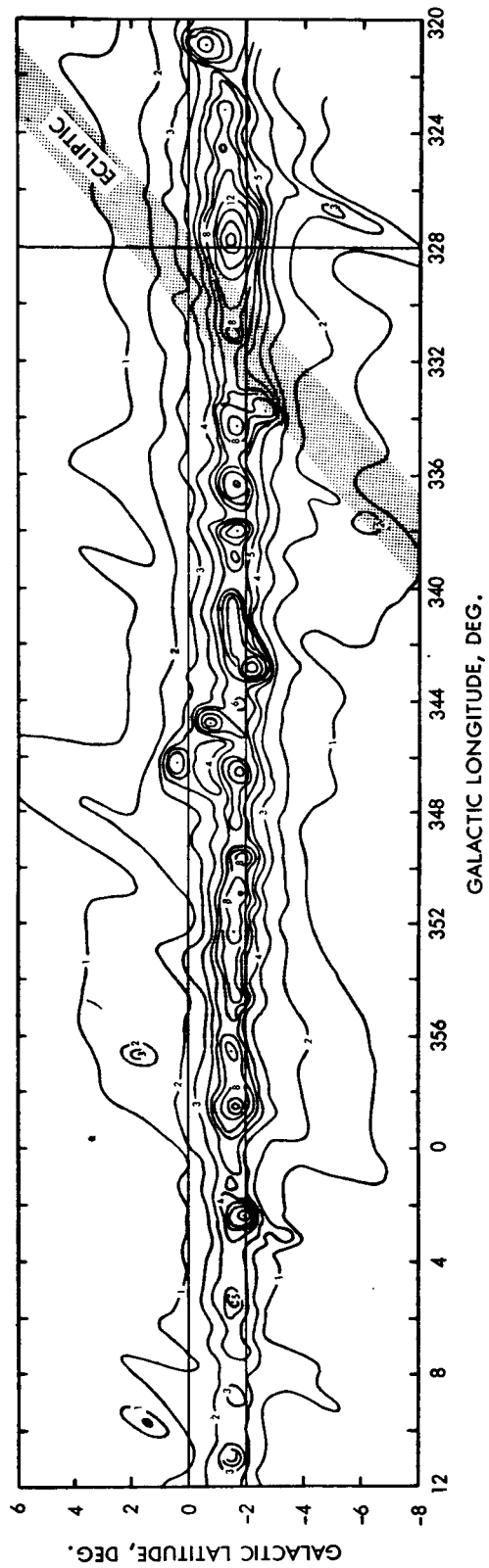


Figure 13b—The same region of the galaxy as shown in Figure 13a to the same scale as observed on 22 cm by Westerhout. The contour unit is 3.25° K. Compare the two maps in the regions of the galactic center (longitude 327.7°); also note the large number of discrete sources superimposed on the background, some of which appear on both maps.

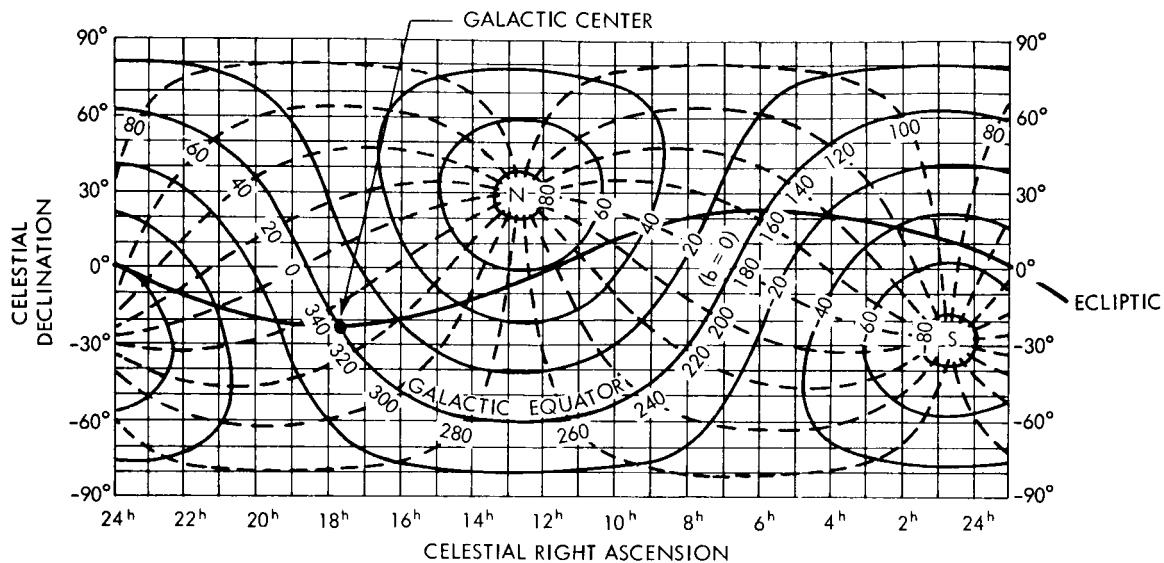


Figure 14—A chart to convert from equatorial to galactic coordinates or vice versa (epoch 1900).

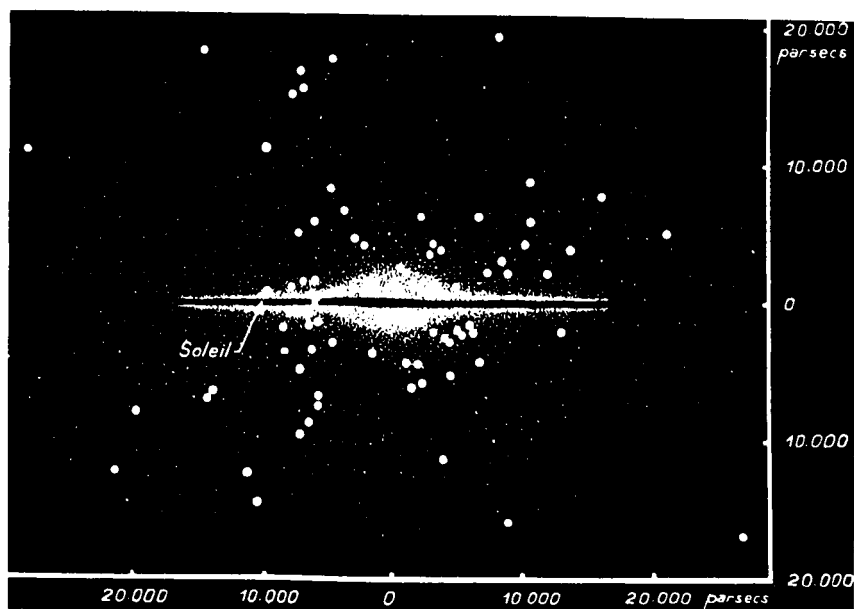
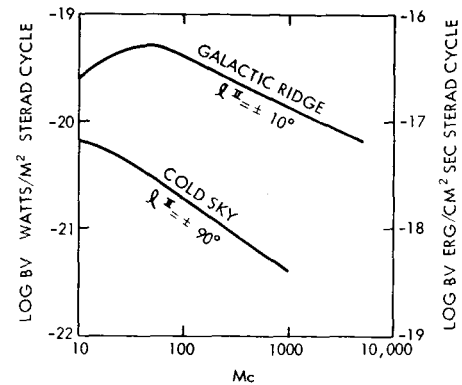


Figure 15—Diagram, due to Plaskett, illustrating the size and shape of the galaxy and the position of the sun. The large white dots represent the globular clusters (Rudaux and de Vaucouleurs, 1948).

Figure 16—Intensity of general cosmic radio emission [1, 7, 11, 12]. General galactic radio emission is concentrated along the galactic equator and towards the galactic center. Measurements are disturbed by irregularities and superimposed sources. We chose as representative regions the galactic ridge at $l^{\text{II}} = \pm 10^\circ$ (i.e. avoiding the Sgr A source), and the coldest part of the sky near $b^{\text{II}} = \pm 90^\circ$.



Let us consider the effect of the galactic noise, when an antenna is pointed into the sky. Assuming two types of antennae (2000 Mc) the received energy flux in the main loop can easily be calculated from Figure 17. The table on the next side gives the fluxes, if the antennas are pointed in either the galactic ridge, the coldest spot in the sky or the moon.

ν	λ	Galactic ridge $l^{\text{II}} = \pm 10^\circ$		Cold sky $b^{\text{II}} = \pm 90^\circ$	
		log T	log I_ν	log T	log I_ν
Mc/s	cm	in °K	in watt m^{-2} (c/s) $^{-1}$ sterad $^{-1}$	in °K	in watt m^{-2} (c/s) $^{-1}$ sterad $^{-1}$
10	3000	5.9	-19.6	5.3	-20.2
20	1500	5.5	-19.4	4.6	-20.3
50	600	4.8	-19.3	3.56	-20.55
100	300	4.09	-19.42	2.76	-20.75
200	150	3.36	-19.55	1.98	-20.93
500	60	2.37	-19.74	0.94	-21.17
1000	30	1.64	-19.87	0.1	-21.4
2000	15	0.9	-20.0		
5000	6	-0.1	-20.2		

Figure 17

Dish	85'	30'
Beamwidth	0,4°	1°
Solid Angle (Steradians)	$3,6 \cdot 10^{-5}$	$2,3 \cdot 10^{-4}$
Minimum detectable energy flux (erg/sec cycle)	$5 \cdot 10^{-20}$	$4 \cdot 10^{-19}$
Effective area A, m ²	290	36,2
Flux density P within solid angle (erg/cm ² sec cycle):		
a. Cold sky	$9 \cdot 10^{-24} ?$	$6 \cdot 10^{-23} ?$
b. Galactic ridge	$3,6 \cdot 10^{-22}$	$2,3 \cdot 10^{-21}$
Received energy flux S = (1/2) · PA erg/sec cycle:		
a. Cold sky	$1,3 \cdot 10^{-17} ?$	$1,4 \cdot 10^{-17} ?$
b. Galactic ridge	$5,2 \cdot 10^{-16}$	$4 \cdot 10^{-16}$
Thermal Radiation from the moon only:		
Flux density P within solid angle (erg/cm ² sec cycle):		
Maximum	$1,9 \cdot 10^{-20}$	$3,1 \cdot 10^{-20}$
Minimum	$5 \cdot 10^{-21}$	$8 \cdot 10^{-21}$
Received energy flux from thermal radiation of the moon (erg/sec cycle) S = (1/2) · PA		
Maximum temperature 390°K	$2,8 \cdot 10^{-14}$	$5,5 \cdot 10^{-15}$
Minimum temperature 100°K	$7 \cdot 10^{-15}$	$1,4 \cdot 10^{-15}$

DISCRETE SOURCES OF COSMIC RADIO WAVES (References 12, 14 and 15)

Within the Galaxy

On top of the galactic continuum dealt with in the preceding chapter, various radio sources are superimposed, some compact, some extended and some of relatively high intensity. At 1963 only 500 strongest sources (galactic and extra-galactic) could be considered as certain. They are not distributed uniformly, but show an obvious concentration along the galactic plane. Stars themselves are not sufficiently strong radio wave emitters to be detectable, at least at 1963. However, some sources have an optical counterpart. About 50 sources have been identified with galactic objects and 60 at least with external galaxies.

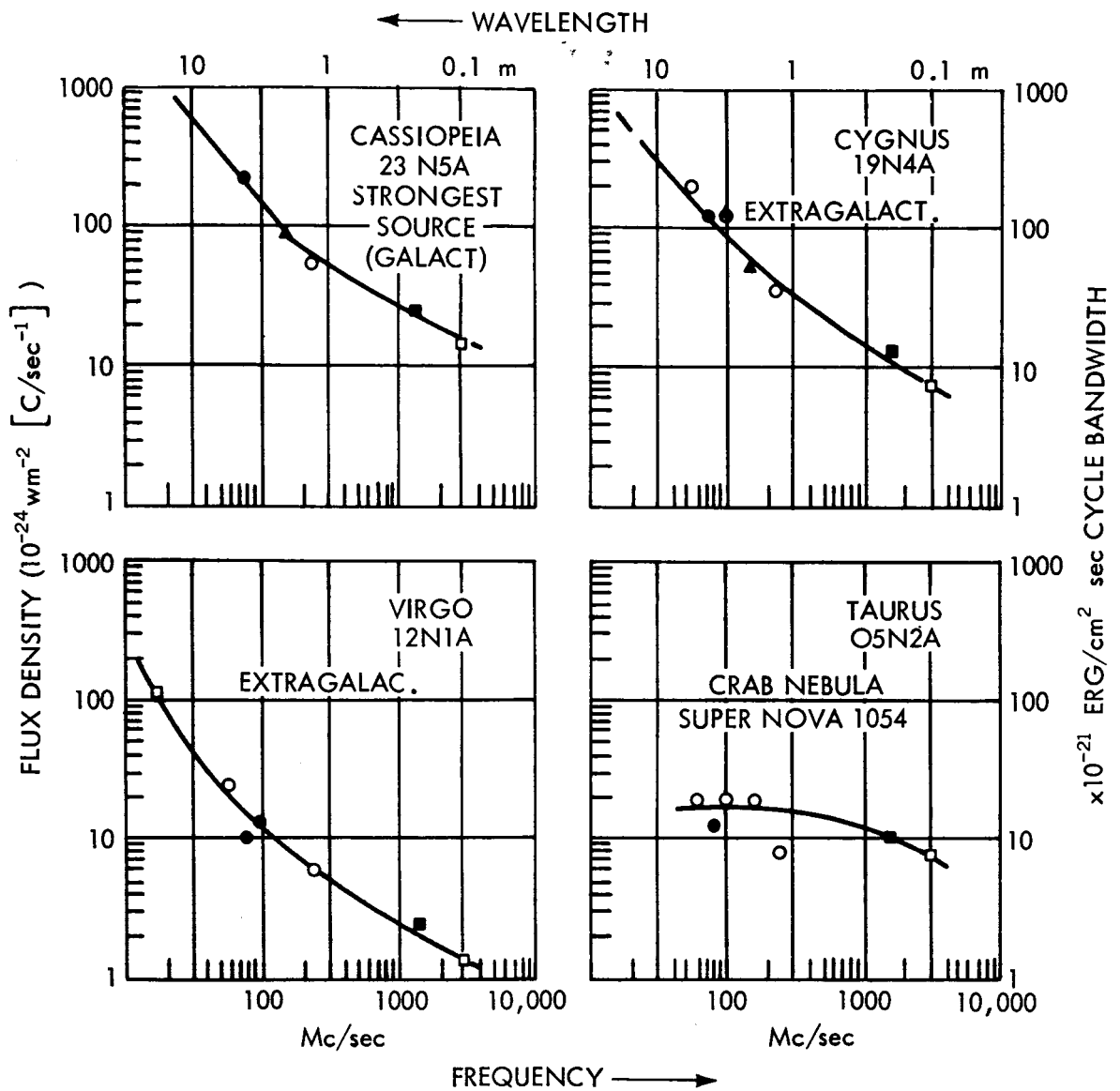


Figure 18—Provisional radio-frequency spectra of the four principal sources as compiled by Wild.

External Galaxies (References 12 and 15)

Two types of galaxies are conveniently distinguished: normal galaxies and radio galaxies, the latter having a much higher intensity.

Normal Galaxies. Our galaxy, Andromeda nebula, Magellanic Clouds, etc.

Radio Galaxies. Cygnus A, Virgo A, etc. Most of them seem to have a double structure.

Radio Emission from Clusters of Galaxies

Emission has been established. Only limited data available. Intensity very low.

Conclusion about Discrete Sources

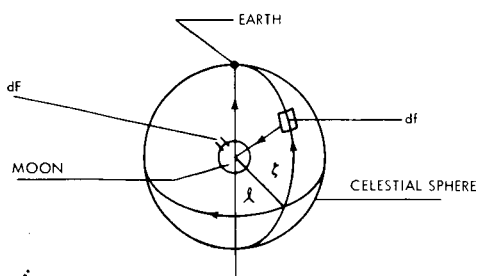
From these figures it can be stated that the flux density (300-3000 Mc) also from the strongest radio source is lower by roughly two order magnitudes than the thermal radiation from the sun and can therefore be neglected.

REFLECTION OF COSMIC RADIO WAVES ON THE MOON SURFACE

Continuum

The flux density on the earth surface, of the reflected cosmic radio waves should be called S_{mr} . Using the coordinate system, shown below and designating the distribution of the cosmic radio waves on the celestial sphere $S(\phi, \theta)$, then S_{mr} becomes:

$$S_{mr} = \frac{1}{4\pi d^2} \int_{\theta=-\frac{\pi}{2}}^{\theta=+\frac{\pi}{2}} \int_{\phi=0}^{\phi=2\pi} \sigma_{(90-\theta)} S(\phi, \theta) [1 + \sin \theta] \frac{r^2 \pi/2}{r^2 \pi} \cos \theta d\phi d\theta$$



$$df = \cos \theta d\phi d\theta$$

$$dF = (1 + \sin \theta) \cdot r^2 \pi/2 \cdot \sigma(90^\circ - \theta) \cdot /4\pi d^2$$

dF the projected illuminated area of the moon by radiation coming from df .

$\sigma(90^\circ - \theta)$. . reflection cross section of the moon surface for an angle of $90 - \theta$ for the incident and reflected beam.

d distance earth/moon.

r diameter of the moon.

Figure 19

However, $S(\phi, \theta)$ is not known on the entire celestial sphere, and the same is the case for $\sigma_{(90^\circ - \theta)}$. So an exact evaluation of the formula above is not possible.

We can however make a rough estimate. As it has been pointed out, only the echo cross section is known and—since this is the largest—we can substitute this value, when establishing an upper limit. The galactic radio emission is concentrated along the galactic equator. The whole 1/2 width of the galactic strip is $3,5^\circ$ for 100 Mc., and for 2000 Mc. it is smaller. The values of Figure 17 refer to the strip $\ell^{II} = \pm 10^\circ$. So, let us assume more or less arbitrary 20° for the width of the galactic strip and the value of the flux density of Figure 17.

The reflected flux density S'_{mr} from this strip becomes:

$$S'_{mr} \sim \frac{20 \cdot \pi}{180} \cdot \pi \cdot 10^{-17} \cdot 3.8 \cdot 10^{-7} \sim 4 \cdot 10^{-24} \text{ erg/cm}^2 \text{ sec cycle}$$

bandwidth for 2000 Mc

The flux density S''_{mr} from the other part of the sky is difficult to estimate, since only the intensity of the coldest spot is known. However, it is established that the flux density does not vary significantly beyond the plane of the galaxy, so that any estimate will not be wrong by the orders of magnitudes.

$$S''_{mr} \sim 2\pi \cdot 2.5 \cdot 10^{-19} \cdot 3.8 \cdot 10^{-7} \sim 6 \cdot 10^{-24} \text{ erg/cm}^2 \text{ sec cycle}$$

bandwidth for 2000 Mc.

So the total (from the moon) reflected flux density $S_{mr} = S'_{mr} + S''_{mr}$ from the cosmic radio waves becomes:

$$S_{mr} \sim 10^{-23} \text{ erg/cm}^2 \text{ sec cycle bandwidth for 2000 Mc.}$$

This value, compared with the thermal radiation of the moon is smaller by a factor of more than 1000.

Discrete Sources

The flux density at 2000 Mc of discrete sources is only known for these of Figure 18. Figure 17 lists the flux density of 25 sources at a frequency of 1000 Mc. The total flux density S_D of these sources is $1.5 \cdot 10^{-20}$ erg/cm² sec cycle bandwidth. The reflected flux density, S_{DR} , if all sources are assumed to be in a position to yield maximum flux density, would be:

$$S_{DR} \sim 1.5 \cdot 10^{-20} \cdot 3.8 \cdot 10^{-7} \sim 6 \cdot 10^{-27} \text{ erg/cm}^2 \text{ sec cycle bandwidth}$$

Though only 25 sources (the most significant) are taken into account, this term can be disregarded with respect to S_{mr} , also if the number of sources is increased.

FINAL REMARKS

It has been shown that for the problem described at the beginning, only the thermal radiation of the moon surface plays an appreciable role.

Lack of exact data calls for reasonable estimates.

Polarization effects, the thermal radiation from stars and radiation from the planets, have for obvious reasons been disregarded.

REFERENCES

1. Pawsey, J. L. and R. N. Bracewell, "Radioastronomie," Oxford at the Clarendon Press, 1955.
2. Baldwin, R. B., "The Measure of the Moon," The University of Chicago Press, p. 268, 1963.
3. Flügge, S.F., "Handbuch der Physik," Bd. 52.
4. Verlag, Springer, "Taschenbuch der Hochfrequenz Technik," Meinke Gundlach, 1962.
5. Börnstein, Landold, "Zahlenwerte u. Funktionen," Vol III, p. 331-352.
6. Bremmer, H., Dr., "Terrestrial Radio Waves," Elsevier Publishing Company, 1949.
7. Evans, J. V., "The Scattering of Radio Waves by the Moon," Proc. Phys. Soc. B. London 70, 1105-1112, 1957.
8. Trexler, J. H., "Lunar Radio Echoes," Proc. Inst. Radio Engrs. 46, 286-292, 1958.
9. Yaplee, B. S., "Radar Echoes from the Moon at a Wavelength of 10 cm.," Proc. Inst. Radio Engrs. 46, 293-297, 1958.
10. Siegel, "Radar Reflection Characteristics of the Moon," p. 29, Paris Symposium on Radio Astronomy, 1959, edited by Bracewell, Stanford University Press.
11. Kuiper, "Planets and Satellites," Vol. 3, The University of Chicago Press, 1961.
12. Steinberg, J. L. and J. Lequeux, "Radio Astronomie," McGraw Hill, 1960.
13. Palmer, H. P., "Radio Astronomy Today," Harvard University Press, 1963.
14. Allen, C. W., "Astrophysical Quantities," University of London, the Athlone Press, 1963.
15. Flügge, S. F., "Handbuch der Physik," Bd. 53.

APPENDIX I

THE POWER REFLECTION COEFFICIENT ρ

ρ depends on the polarization of the incident wave and is described by Fresnel's formulas:

$$\rho = \frac{(\text{reflected field strength})^2}{(\text{incident field strength})^2}$$

For vertical polarization (field strength in plane of incidence):

$$\rho_{\perp} = \frac{(Z_1 \cos \alpha_1 - Z_2 \cos \alpha_2)^2}{(Z_1 \cos \alpha_1 + Z_2 \cos \alpha_2)^2}$$

For horizontal polarization (field strength vertical to plane of incidence):

$$\rho_{\parallel} = \frac{(Z_2 \cos \alpha_1 - Z_1 \cos \alpha_2)^2}{(Z_2 \cos \alpha_1 + Z_1 \cos \alpha_2)^2}$$

Z_1, Z_2 = wave resistance of the upper and lower medium.

$\alpha_2 \dots \sin \alpha_2 = Z_2 (\sin \alpha_1) / Z_1$ Snellius

$$Z = \sqrt{\frac{\mu_0 \mu_r}{\epsilon_0 (\epsilon_r - fK/\omega\epsilon_0)}}$$

$$\epsilon_0 = 8,855 \cdot 10^{-12} \text{ F/m}$$

$$\mu_0 = 4\pi \cdot 10^{-7} \text{ H/m}$$

μ_r, ϵ_r relative permeability and dielectric constant respectively

K conductivity

$\omega = 2\pi/f, f$. . . frequency

α_1, α_2 are defined in Figure 20.

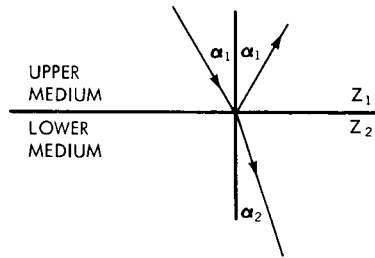


Figure 20

In the case of interest, the upper medium is vacuum and Z_1 becomes:

$$Z_1 = 377 \Omega$$

In the case of the moon surface K, ϵ_r, μ_r are not known.

However, these quantities could be determined by analogy with dry materials on earth.

A survey about K, ϵ_r, μ_r for a large number of soils and stones is given in Reference 5.

Reference 10 gives a more recent summary.

CONCLUSIONS

- a. K depends strongly on the humidity. The term $K/\omega\epsilon_0$ can be neglected in comparison with ϵ_r for 2,000 Mc. A typical value K for dry soil, as it could be expected on the moon surface, would be $K \sim 10^{-3} \Omega^{-1} \text{m}^{-1}$, resulting in $K/\omega\epsilon_0 \sim 10^{-2} \ll \epsilon_r$ for 2,000 Mc. This is the reason why every soil behaves as a dielectric at high frequencies, while it behaves as a conductor at low frequencies.

b. $\mu = 1$ for all kinds of soils and stones.

c. Typical static values of ϵ_r for dry soils lie between 7-16 (Reference 5). But Bremmer (Reference 6) gives $E_r = 4$ for an average soil. (See also Reference 10.) ϵ_r increases with an increasing humidity. Above 300 Mc the static values for soil are no longer valid, but decrease slowly to about 2 (Reference 4). Data showing the dependence of ϵ_r on the frequency for the materials of interest could not be found.

Figure 21, a and b, give the power reflection coefficient for $K = 0$, $\mu = 1$, $\epsilon_r = 17, 7, 4$ as a function of α_1 , the angle of incidence. $\rho_{||}$ and ρ_{\perp} are power reflection coefficients for parallel and vertical polarization respectively.

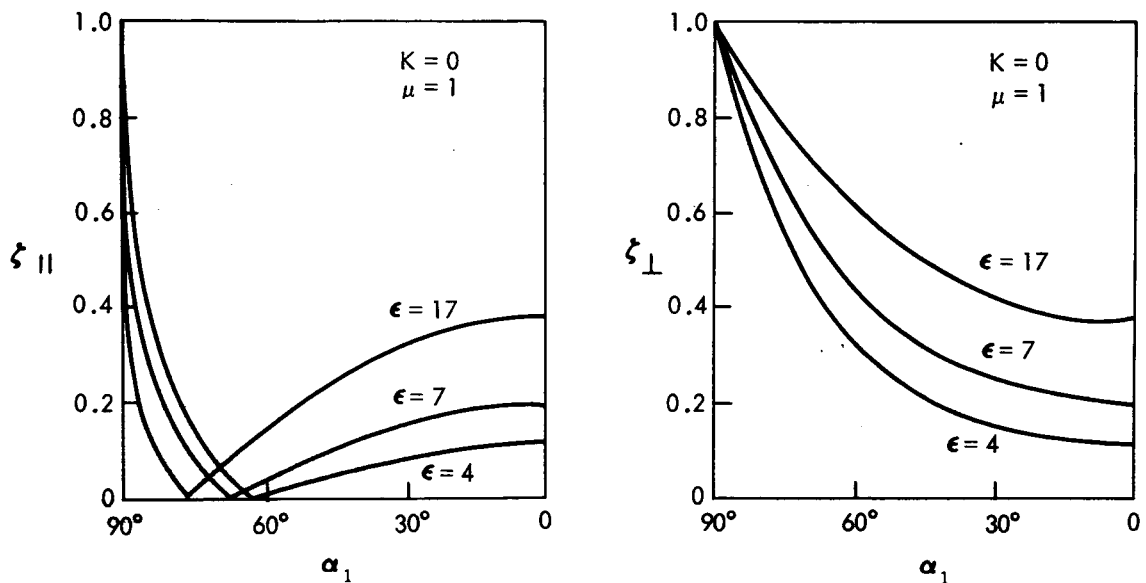


Figure 21

In the case of reflection of a blank sphere in the direction $(2\alpha_1, \phi)$ we have the case as shown in Figure 22.

The reflection coefficient ρ in the direction $2\alpha_1$ for an arbitrary ϕ and unpolarized radiation becomes then:

$$\rho = (1/2) (\rho_{||} + \rho_{\perp}) \cos \alpha_1$$

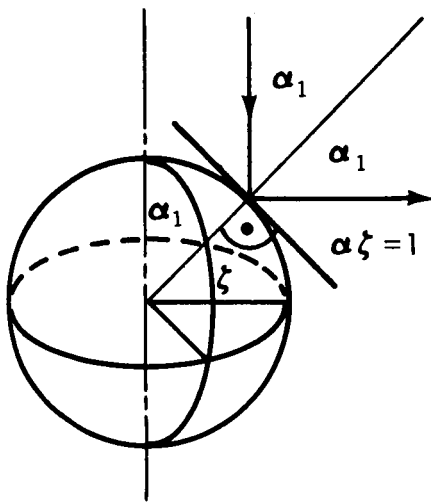


Figure 22

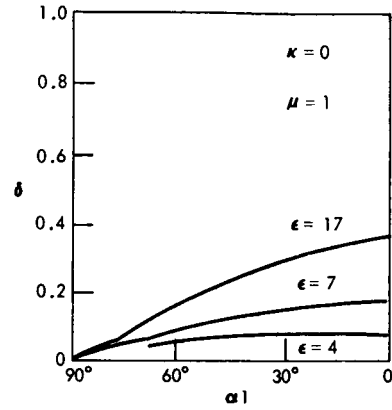


Figure 23

In Figure 23, ρ is plotted for $\epsilon_r = 17, 7, 4, K = 0$. Thus the power reflection coefficient for unpolarized radiation and for the materials of interest is the largest for vertical incidence (reflection on a blank sphere).